morphology contradicts Rak's dichotomization of East and South African robust *Australopithecus*[6].

It is possible that the KGA *A. boisei* population as a whole was morphologically distinct from that of the Turkana basin, despite a geographical proximity of approximately 200 km. The Konso macromammalian fauna exhibits significant differences from the Turkana counterparts at both 1.4 Myr and 1.9 Myr levels. Dominant bovids and suids at Konso include *Kobus* cf. *sigmoidalis*, *Damaliscus niro*, *Parmularius angusticornis*, a short-horned *Syncerus*, *Tragelaphus strepsiceros*, *Kolpochoerus majus*, *Kolpochoerus limnetes/olduvaiensis*, *Notochoerus* aff. *euilus*, and *Metridiochoerus hopwoodi*. Most of these taxa are rare or absent at equivalent Turkana time horizons, or are different at the infraspecific level[17,18]. Similarly, the abundant Acheulean assemblages found at KGA are lacking at East Turkana[19]. Thus, distinct differences between Konso and Turkana are seen in *A. boisei*, the fauna and archeological remains. Because all *Australopithecus* species hypodigms come from one dominant and a few subsidiary site samples, the extent of the polytypic nature of early hominid species may have been overlooked.

The importance of the Konso *A. boisei* fossils lies in their possession of uniquely derived features of that species, thus allowing secure taxonomic attribution at the species level, while otherwise extending the known range of *A. boisei* variation in many features. The striking deviations of the Konso morphology from the known Olduvai/Turkana *A. boisei* condition demonstrate that not all *A. boisei* features traditionally considered as part of a hyper-robust masticatory adaptation are of functional significance or decisive systematic value. This has important implications for early-hominid systematics and functional interpretations.

It is likely that many details of craniodental features used in evaluations of early hominids vary between populations in a manner consistent with random genetic drift. Excessive atomization of morphological features and their individual evaluations may then lead to erroneous phylogenetic and simplistic functional interpretations. We hypothesize that the facial morphology of the Konso skull, unique in the known *A. boisei* hypodigm, represents intraspecific variation, either individual, age-related, temporal and/or geographic. The striking distinctiveness of the Konso skull and the morphological trends common to both palates (KGA10-506 and KGA10-525) suggest that geographic variation is particularly influential. Geographically patterned, inter-basinal variation may be revealed further as more *A. boisei* specimens become available. Meanwhile, as some features once thought to characterize South African *A. robustus* are now shown to occur in East Africa, the case for robust *Australopithecus* monophyly is strengthened.

The taxonomic splitting of the ~2.0-Myr early-*Homo* hypodigm is a scheme rapidly gaining wide acceptance[20–23], and the newly proposed taxon *Australopithecus bahrelghazali* has been claimed to be distinct from *A. afarensis*[24]. These interpretations rely heavily on specimen-specific morphological differences. Such differences have been taken as indicating cladogenesis, but the Konso discoveries combined with modern anthropoid variation[25,26] suggest that considerable morphological polymorphism and/or polytypism may have been present among all early hominids. Splitting of taxa at the species level, emphasizing minor morphological differences, would then be unwarranted. We predict that, as new hominid-bearing sedimentary basins are discovered and existing site samples are augmented, a more accurate picture of variation will emerge to challenge overly split phylogenies of hominid species. □

Received 10 June; accepted 9 September 1997.

1. Leakey, L. S. B. A new fossil skull from Olduvai. *Nature* **184,** 491–493 (1959).
2. Tobias, P. V. T. *Olduvai Gorge* Vol. 2, *The Cranium and Maxillary Dentition of* Australopithecus (Zinjanthropus) boisei (Cambridge Univ. Press, 1967).
3. Leakey, R. E. F. & Walker, A. New *Australopithecus boisei* specimens from East and West Lake Turnaka, Kenya. *Am. J. Phys. Anthropol.* **76,** 1–24 (1988).
4. Wood, B. Koobi Fora Research Project Vol. 4 *Hominid Cranial Remains* (Clarendon, Oxford, 1991).
5. Brown, B., Walker, A., Ward, C. V. & Leakey, R. E. New *Australopithecus boisei* calvaria from East Lake Turkana, Kenya. *Am. J. Phys. Anthropol.* **91,** 137–159 (1993).
6. Rak, Y. *The Australopithecine Face* (Academic, New York, 1983).
7. Shipman, P. & Harris, J. M. in *Evolutionary History of the "Robust" Australopithecines* (ed. Grine, F.) 343–381 (de Gruyter, New York, 1988).
8. Asfaw, B. *et al.* The earliest Acheulean from Konso-Gardula. *Nature* **360,** 732–735 (1992).
9. Holloway, R. L. Human paleontological evidence relevant to language behaviour. *Hum. Neurobiol.* **2,** 105–114 (1983).
10. Suwa, G., White, T. D. & Howell, F. C. Mandibular postcanine dentition from the Shungura Formation, Ethiopia: Crown morphology, taxonomic allocations, and Plio-Pleistocene hominid evolution. *Am. J. Phys. Anthropol.* **101,** 247–282 (1996).
11. Walker, A., Leakey, R. E., Harris, J. M. & Brown, F. H. 2.5-Myr *Australopithecus boisei* from west of Lake Turkana. *Nature* **322,** 517–522 (1986).
12. Carney, J., Hill, A., Miller, J. & Walker, A. Late australopithecine from Baringo district, Kenya. *Nature* **230,** 509–514 (1971).
13. Gowlett, J. A. J., Harris, J. W. K., Walton, D. & Wood, B. A. Early archaeological sites, hominid remains and traces of fire from Chesowanja, Kenya. *Nature* **294,** 125–129 (1981).
14. Leakey, L. S. B. & Leakey, M. D. Recent discoveries of fossil hominids in Tanganyika at Olduvai and near Lake Natron. *Nature* **202,** 5–7 (1964).
15. Thouveny, N. & Taieb, M. Etude paleomagnetique des formations du Plio-Pleistocene de la Peninj (ouest du lac Natron, Tanzanie), limites de l'interpretation magnetostratigraphique. *Sci. Geol. Bull.* **40,** 57–70 (1987).
16. Wood, B., Wood, C. & Konigsberg, L. *Paranthropus boisei*: An example of evolutionary stasis? *Am. J. Phys. Anthropol.* **95,** 117–136 (1994).
17. Harris, J. M. *Koobi Fora Research Project* Vol. 2, *The Fossil Ungulates: Proboscidea, Perissodactyla, and Suidae* (Clarendon, Oxford, 1983).
18. Harris, J. M. *Koobi Fora Research Project* Vol. 3, *The Fossil Ungulates: Geology, Fossil Artiodactyls and Palaeoenvironments* (Clarendon, Oxford, 1991).
19. Leakey, M. G. & Leakey, R. E. *Koobi Fora Research Project* Vol. 1, *The Fossil Hominids and an Introduction to Their Context, 1968–1974* (Clarendon, Oxford, 1978).
20. Wood, B. Origin and evolution of the genus *Homo*. *Nature* **355,** 783–790 (1992).
21. Rightmire, G. P. Variation among early *Homo* crania from Olduvai Gorge and the Koobi Fora region. *Am. J. Phys. Anthropol.* **90,** 1–33 (1993).
22. Schrenk, F., Bromage, T. G., Betzler, C. G., Ring, U. & Juwayeyi, Y. Oldest *Homo* and Pliocene biogeography of the Malawi rift. *Nature* **365,** 833–836 (1993).
23. Kimbel, W. H., Johanson, D. C. & Rak, Y. Systematic assessment of a maxilla of *Homo* from Hadar, Ethiopia. *Am. J. Phys. Anthropol.* **103,** 235–262 (1997).
24. Brunet, M. *et al. Australopithecus bahrelghazali*, une nouvelle espace d'Hominide ancien de la region de Koro Toro (Tchad). *C. R. Acad. Sci.* **322,** 907–913 (1996).
25. Albrecht, G. H. & Miller, J. in *Species, Species Concepts, and Primate Evolution* (eds Kimbel, W. H. & Martin, L. B.) 123–161 (Plenum, New York, 1993).
26. Uchida, A. *Peabody Museum Bulletin 4. Intra-species Variation among the Great Apes: Implications for Taxonomy of Fossil Hominoids* (Harvard Univ. Press, Cambridge, MA, 1996).
27. du Brul, E. L. Early Hominid feeding mechanisms. *Am. J. Phys. Anthropol.* **47,** 305–320 (1977).
28. Kimbel, W. H., White, T. D. & Johanson, D. C. in *Evolutionary History of the "Robust" Australopithecines* (ed. Grine, F.) 259–268 (de Gruyter, New York, 1988).
29. McCollum, M. A., Grine, F. E., Ward, S. C. & Kimbel, W. H. Subnasal morphological variation in extant hominoids and fossil hominids. *J. Hum. Evol.* **24,** 87–111 (1993).
30. WoldeGabriel, G. *et al.* Ecology and temporal placement of early Pliocene hominids at Aramis, Ethiopia. *Nature* **371,** 330–333 (1994).

Acknowledgements. The Konso Paleoanthropological Research Project has been conducted under permission from the Center for Research and Conservation of Cultural Heritage (CRCCH), Ministry of Information and Culture, Ethiopia. We thank the CRCCH and the National Museum of Ethiopia for allowing us to undertake our research; the Bureau of Culture and Information of the Southern Nations, Nationalities, and People's regional Government of Ethiopia for support; staff of the Bureau of Culture and Information and of CRCCH for participating in and contributing to the field research; A. Amzaye for discovering the KGA10-525 skull; the administration of the Konso Special Administration District and the Konso people for their support; A. Ademassu, T. Assebewerk, T. Becker, H. Gilbert, C. Guillemot, Y. Haile-Selassie, F. C. Howell, B. Latimer, S. Simpson, M. Umer and Y. Zeleke for field participation, laboratory assistance, and/or suggestions; P. Snow for access to the LANL Geology/Geochemistry Group microprobe facility and assistance; and R. Holloway for the cranial-capacity estimate of KGA10-525. This work was funded by the Mitsubishi Foundation and the Japan Ministry of Education, Science, Sports and Culture.

Correspondence and requests for materials should be addressed to G.S. (suwa@biol.s.u-tokyo.ac.jp).

Decrease of cardiac chaos in congestive heart failure

Chi-Sang Poon & Christopher K. Merrill

Harvard-MIT Division of Health Sciences and Technology, Massachusetts Institute of Technology, Cambridge, Massachusetts 02139, USA

The electrical properties of the mammalian heart undergo many complex transitions in normal and diseased states[1–7]. It has been proposed that the normal heartbeat may display complex nonlinear dynamics, including deterministic chaos[8,9], and that such cardiac chaos may be a useful physiological marker for the diagnosis[10–12] and management[13,14] of certain heart trouble. However, it is not clear whether the heartbeat series of healthy and diseased hearts are chaotic or stochastic[15–17], or whether cardiac chaos represents normal or abnormal behaviour[18]. Here we have used a highly sensitive technique, which is robust to random noise, to detect chaos[19]. We analysed the electrocardiograms from a group of healthy subjects and those with severe congestive heart failure (CHF), a clinical condition associated with a high risk of

Nature © Macmillan Publishers Ltd 1997

sudden death. The short-term variations of beat-to-beat interval exhibited strongly and consistently chaotic behaviour in all healthy subjects, but were frequently interrupted by periods of seemingly non-chaotic fluctuations in patients with CHF. Chaotic dynamics in the CHF data, even when discernible, exhibited a high degree of random variability over time, suggesting a weaker form of chaos. These findings suggest that cardiac chaos is prevalent in healthy heart, and a decrease in such chaos may be indicative of CHF.

One of the main problems in studying the nonlinear dynamical behaviour of the heartbeat (and of any empirical time series in general) is the inevitable presence of random noise, which can often lead to false positive or negative identifications of chaos when traditional methods of nonlinear dynamics analysis are used. Although the effect of noise may be lessened to some extent by using long data records, this approach is limited by the possible non-stationarity of the heartbeat series[20,21].

To circumvent these difficulties, we have used a nonlinear systems identification technique[19] to detect time-dependent and disease-dependent changes in the chaotic dynamics of the heartbeat. The technique identifies nonlinear determinism in a time series by iteratively generating a family of polynomial autoregressive models. The null hypothesis (namely, that the time series is stochastic with linear dynamics) is rejected if there is at least one nonlinear model that provides a significantly better fit to the data in a parsimonious manner than linear autoregressive models of all dynamical order. The statistical test is highly robust and sensitive, in that it is resistant to noise contamination and is applicable to short time series (with $<$1,000 points). This technique provides a highly specific test for deterministic chaos in that the null hypothesis is not readily rejected in the presence of random noise unless the underlying system is chaotic and/or has a fractal phase-space structure[19]. Indeed, simulation studies showed that the level of noise corruption that could be tolerated by such a chaotic test was directly related to the magnitude of the positive Lyapunov exponent, a measure of the degree of chaos in the underlying noise-free data (M. Barahona and C.-S.P., unpublished observations). Moreover, the computational algorithm uses a recursive scheme for nonlinear systems identification and is highly efficient (typically, analysis of a 1,000-point time series takes just seconds on a desktop computer). The combination of specificity, sensitivity and computational efficiency of the chaotic test allowed a systematic statistical evaluation of the presence of deterministic chaos in multiple short segments of an extended heartbeat series, an analytical approach that would otherwise be impractical.

The data sets of interest were derived from an established database[17,20,22] and consisted of continuous Holter records (at 128–250 samples s^{-1}) of heartbeat intervals from 8 healthy subjects and 11 CHF patients (age range, 22–71 years). At the time of the experiment, none of the subjects was on any medication that would affect the heart rate. To obviate possible non-physiological disturbances associated with wakefulness, data obtained only during nocturnal hours (totally 20,000 beats each) were used in the analysis. Subjects in both groups were selected on the basis of stability of the mean heart rate and limited number of ectopic beats and undetected beats. The heartbeat series were detrended using linear regression, but otherwise no preprocessing of the data was performed.

The heartbeat series of the CHF patients were characterized by the distinct presence of low-amplitude, low-frequency intermittent oscillations and decrease in temporal variability (Fig. 1), as reported previously[22,23]. Generally, such an increase in regularity and decrease in temporal variability may reflect a decrease in either the noise or chaotic contents of the time series. To distinguish these possibilities, we first divided each heartbeat series into 40 contiguous short segments (of 500 beats each) to minimize the effect of non-stationarity of the data. We then applied the chaotic test to each data segment and evaluated the frequencies of linear and nonlinear episodes in each subject.

Nonlinear dynamics were manifested under the above test in both healthy and CHF heartbeat data (Fig. 2a, b). Because the chaotic test is conservative in the presence of noise (that is, predisposing to a

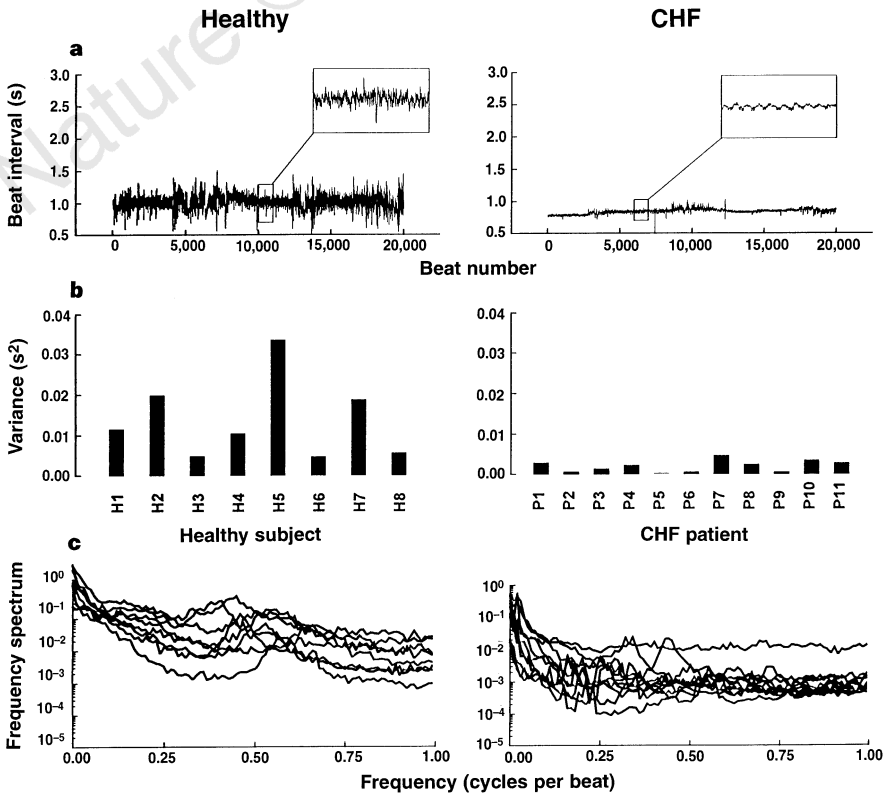

Figure 1 Characteristics of heartbeat data. **a**, Representative heartbeat series from a healthy subject (left) and a CHF patient (right). All heartbeat data were obtained during sleep and consisted of 20,000 beats. Insets show the self-similar character of the healthy heartbeat series and the decreased complexity and increased predictability of the CHF data in the form of low-amplitude, low-frequency intermittent oscillations. **b**, Variance of heartbeat intervals in all healthy subjects (left) and all CHF patients (right). Note the decreased variability of heartbeat in the CHF patient. **c**, Frequency spectrum of heartbeat intervals in all healthy subjects (left) and all CHF patients (right). Each frequency spectrum was obtained by taking a 2,000-point Fourier transform of the corresponding heartbeat series, averaged over all data segments, and then integrated over a 10-point bin in the frequency scale. The lack of sustained periodic or quasiperiodic components is indicated by the absence of frequency peaks in both subject groups.

Nature © Macmillan Publishers Ltd 1997

Nature © Macmillan Publishers Ltd 1997

linear model unless the data have a significant chaotic component), this finding suggests that the heartbeat series were intrinsically chaotic in both subject groups. The absence of other forms of nonlinear dynamics (such as limit cycles or invariant loops) is also indicated by the lack of constantly periodic or quasiperiodic components in the heartbeat series and corresponding frequency spectrum of all subjects (Fig. 1). Furthermore, the possible contribution of non-chaotic fractal attractors to the nonlinear dynamics may also be excluded, as such attractors occur only under certain special circumstances[24], which are unlikely in the cardiac system.

However, deterministic chaos was detected consistently in nearly all data segments in the healthy group, but the detection rate was markedly decreased (by 20–80%) in all but one of the CHF patients (Fig. 2b). Because all data were from subjects during nocturnal hours, and the CHF data were even less variable than the normal data (Fig. 1), it is highly unlikely that the low detection rate in the CHF group was caused by increased noise corruption. To confirm this, we repeated the test with data segments of 2,000 beats each to increase the signal content. Again, all healthy heartbeat data with the longer segmentation proved strongly chaotic, but the corresponding CHF data still exhibited relatively low detection rates (Fig. 2c). Because a weakly chaotic time series is generally more susceptible to noise corruption than is a strongly chaotic one (one with a large positive Lyapunov exponent), the low detection rate in the CHF group suggests that the intensity of cardiac chaos was decreased in CHF patients.

Another way of measuring the changes in intensity of chaos in a noise-corrupted time series is to compare the variability of the resulting nonlinear models for those data segments that tested positive for deterministic chaos. Again, we make use of the property that the chaotic dynamics in a noise-corrupted time series is more readily identifiable if it has a higher signal-to-noise ratio. Thus the nonlinear coefficient estimates for the CHF data are expected to be less variable if the lower temporal variability of the CHF data (Fig. 1) reflected a decrease in noise level instead of a decrease in chaotic content.

To test this hypothesis, we computed the nonlinear coefficients for all chaotic segments of the healthy and CHF heartbeat series. Indeed, the estimated nonlinear coefficients were considerably more variable in the CHF patients than in healthy subjects (Fig. 3). This criterion again held in all but one of the CHF patients and for the group as a whole. The increased parameter variability in the CHF group, together with a corresponding decrease in detection rate for

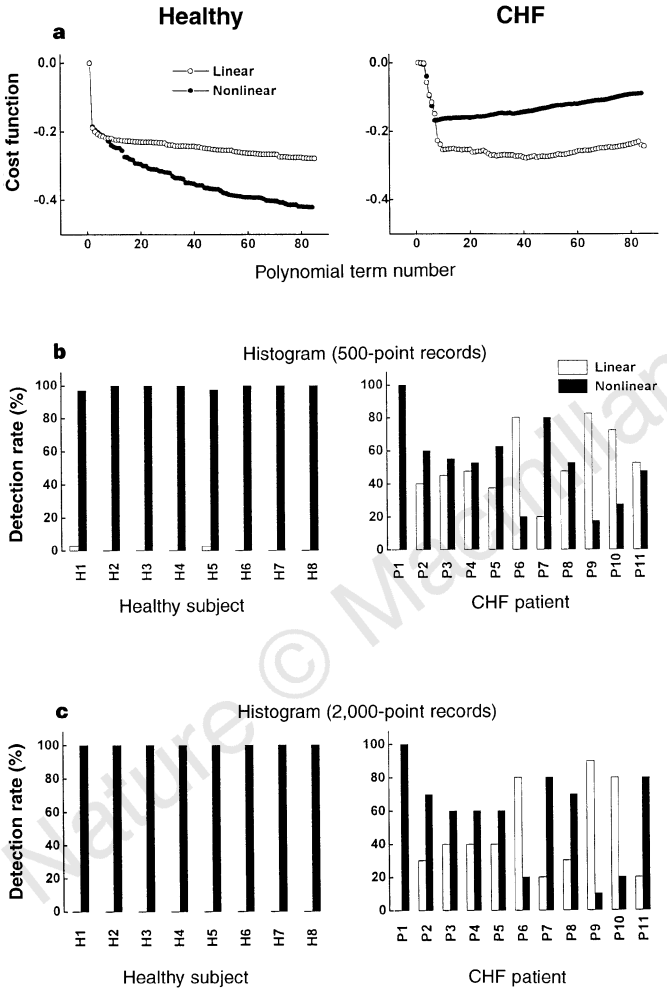

Figure 2 Chaos analysis of heartbeat series. The data were fitted with dynamical models of linear and polynomial forms with increasing order. Nonlinear dynamics was indicated if the best nonlinear model provides a better fit to the data than the best linear model with a similar number of polynomial terms. Model selection was based upon the *F*-ratio test for residuals at the 1% significance level. This technique is conservative in that it predisposes to a linear model (null hypothesis) in the presence of random noise unless the system is chaotic[19]. **a**, Examples of linear and nonlinear model fits of a 500-beat data segment for the same healthy subject (left) and CHF patient (right) shown in Fig. 1a. The cost function is of the form[19]: $C(r) = \log_e \epsilon(r) + r/N$, where r is the number of polynomial terms, $\epsilon(r)$ is the residual error, and N is the length of the time series. Both the cost function and the *F*-ratio test yielded a nonlinear model for the healthy subject and a linear model for the CHF subject. **b**, Histograms of linear and nonlinear model selection for all 500-beat data segments based on the above test in healthy subjects (left) and CHF patients (right). Note the high detection rates for chaos (nearly 100%) in the healthy group and the relatively low detection rates in CHF group (except patient P1). **c**, As **b**, but using 2,000-beat data segments.

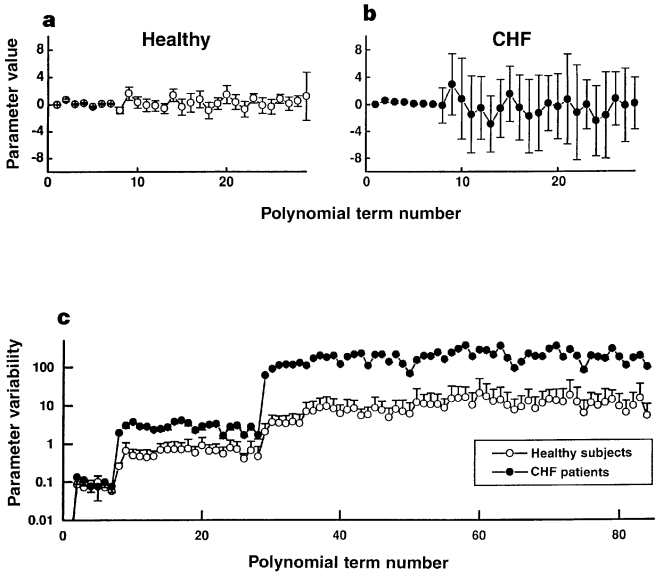

Figure 3 Variability of parameter estimates corresponding to all 500-beat data segments that were identified as chaotic in Fig. 2. Data shown are estimates of the leading nonlinear coefficients (mean ± s.d.) from the same healthy subject (**a**) and CHF patient (**b**) shown in Fig. 1a. Note the increased variability (s.d.) of estimated coefficients in the CHF patient. **c**, Average s.d. values (mean ± s.e.) of the first 80 nonlinear coefficient estimates for the healthy and CHF groups are plotted on a semi-logarithmic scale. The parameter estimates were significantly more variable in the CHF group than in the healthy group. All CHF patients except P1 exhibited similar increased parameter variability.

Nature © Macmillan Publishers Ltd 1997

Nature © Macmillan Publishers Ltd 1997

chaos (Fig. 2), confirm that the degree of cardiac chaos was decreased in the CHF patients.

These critical tests strongly support the suggested prevalence of cardiac chaos in healthy subjects[8,9]. Moreover, our results indicate that cardiac chaos persists in CHF patients, albeit less strongly than in healthy subjects. The intermittent heartbeat oscillations characteristic of these patients[22] (Fig. 1) suggest that they may be at the brink of intermittency, a common route to and out of chaos[25]. Whereas the effect of noise contamination of the data precluded the reliable detection of chaos with previous approaches, we have used this property to evaluate statistically the changes in cardiac chaos with heart disease. Such a statistical approach has been made possible by the sensitivity, specificity and computational efficiency of the chaotic test[19].

Our results do not reveal the mechanisms of cardiac chaos and its recession in heart failure; indeed abnormalities in left ventricular and autonomic system functions may all contribute to a decrease in complexity of the heartbeat nonlinear dynamics in CHF patients[22]. Nevertheless, of all the subjects tested, only one CHF patient failed both diagnostic criteria, corresponding to a type-I and type-II diagnostic error of 9% and 0%, respectively. Such remarkable consistency of the chaotic tests, together with the efficiency of the computational algorithm, suggest that such indices of chaos may be used as a specific, non-invasive and on-line diagnostic test for heart disease, and a possible indicator of imminent ventricular fibrillation[26]. □

Received 20 May; accepted 1 August 1997.

1. Smith, J. M. & Cohen, R. J. Simple finite-element model accounts for wide range of cardiac dysrhythmias. *Proc. Natl Acad. Sci. USA* **81,** 233–237 (1984).
2. Chialvo, D. R. & Jalife, J. Nonlinear dynamics of cardiac excitation and impulse propagation. *Nature* **330,** 749–752 (1987).
3. Chialvo, D. R., Gilmour, R. F. & Jalife, J. Low-dimensional chaos in cardiac tissue. *Nature* **343,** 653–657 (1990).
4. Jalife, J. *Ann. NY Acad. Sci.* **591** (1990).
5. Davidenko, J. M., Pertsov, R. S., Baxter, W. & Jalife, J. Stationary and drifting spiral waves of excitation in isolated cardiac muscle. *Nature* **355,** 349–351 (1989).
6. Winfree, A. T. Electrical turbulence in three-dimensional heart muscle. *Science* **266,** 1003–1006 (1994).
7. Glass, L. Dynamics of cardiac arrhythmias. *Phys. Today* 40–45 (1996).
8. Goldberger, A. L. Is the normal heartbeat chaotic or homeostatic? *News Physiol. Sci.* **6,** 87–91 (1991).
9. Sugihara, G., Allan, W., Sobel, D. & Allan, K. D. Nonlinear control of heart rate variability in human infants. *Proc. Natl Acad. Sci. USA* **93,** 2608–2613 (1996).
10. Denton, T. A., Diamond, G. A., Helfant, R. H., Khan, S. & Karagueuzian, H. Fascinating rhythm: A primer on chaos theory and its application to cardiology. *Am. Heart J.* **120,** 1419–1440 (1990).
11. Skinner, J. E., Goldberger, A. L., Mayer-Kress, G. & Ideker, R. E. Chaos in the heart: Implications for clinical cardiology. *Biotechnology* **8,** 1018–1024 (1990).
12. Goldberger, A. L. Nonlinear dynamics for clinicians: Chaos theory, fractals and complexity at the bedside. *Lancet* **347,** 1312–1314 (1996).
13. Garfinkel, A., Spano, M. L., Ditto, W. L. & Weiss, J. N. Controlling cardiac chaos. *Science* **257,** 1230–1235 (1992).
14. Garfinkel, A., Weiss, J. N., Ditto, W. L. & Spano, M. L. Chaos cotnrol of cardiac arrhythmias. *Trends Cardiovasc. Med.* **5,** 76–80 (1995).
15. Kaplan, D. T. & Cohen, R. J. Is fibrillation chaos? *Circ. Res.* **67,** 886–892 (1990).
16. Kanters, J. K., Holstein-Rathlou, N.-H. & Agner, E. Lack of evidence for low-dimensional chaos in heart rate variability. *J. Cardiovasc. Electrophysiol.* **5,** 591–601 (1994).
17. Turcott, R. G. & Teich, M. C. Fractal character of the electrocardiogram: Distinguishing heart-failure and normal patients. *Ann. Biomed. Eng.* **24,** 269–293 (1996).
18. Glass, L. Is cardiac chaos normal or abnormal? *J. Cardiovasc. Electrophysiol.* **1,** 481–482 (1990).
19. Barahona, M. & Poon, C.-S. Detection of nonlinear dynamics in short, noisy time series. *Nature* **381,** 215–217 (1996).
20. Peng, C. K., Havlin, S., Stanley, H. E. & Goldberger, A. L. Quantification of scaling exponents and crossover phenomena in nonstationary heartbeat time series. *Chaos* **5,** 82–87 (1995).
21. Ivanov, P. C. *et al.* Scaling behaviour of heartbeat intervals obtained by wavelet-based time-series analysis. *Nature* **383,** 323–327 (1996).
22. Goldberger, A. L., Rigney, D. R., Mietus, J., Antman, E. W. & Greenwald, S. Nonlinear dynamics in sudden cardiac death syndrome: heartrate oscillations and bifurcations. *Experientia* **44,** 983–987 (1988).
23. Casolo, G., Balli, E., Taddei, T., Amuhasi, J. & Gori, C. Decreased spontaneous heart rate variability on congestive heart failure. *Am. J. Cardiol.* **64,** 1162–1167 (1989).
24. Grebogi, C., Ott, E., Pelikan, S. & Yorke, J. A. Strange attractors that are not chaotic. *Physica D* **13,** 261–268 (1984).
25. Pomeau, Y. & Manneville, P. Intermittent transition to turbulence in dissipative dynamical systems. *Commun. Math. Phys.* **74,** 189–197 (1980).
26. Skinner, J. E., Pratt, C.-M. & Vybiral, T. A. Reduction in the correlation dimension of heartbeat intervals precedes imminent ventricular fibrillation in human subjects. *Am. Heart J.* **125,** 731–743 (1993).

Acknowledgements. We thank A. L. Goldberger and R. G. Mark for discussions and comments on the manuscript, and A. L. Goldberger and J. E. Mietus for providing the heartbeat data. This work was supported by grants from the National Heart, Lung and Blood Institute, National Science Foundation, and Office of Naval Research.

Correspondence and requests for materials should be addressed to C.-S.P. (e-mail: cpoon@mit.edu).

A specific neural substrate for perceiving facial expressions of disgust

M. L. Phillips*, A. W. Young†, C. Senior*, M. Brammer‡, C. Andrew§, A. J. Calder†, E. T. Bullmore‡, D. I. Perrett‖, D. Rowland‖, S. C. R. Williams§, J. A. Gray¶ & A. S. David*

** Department of Psychological Medicine, King's College School of Medicine and Dentistry and Institute of Psychiatry, 103 Denmark Hill, London SE5 8AZ, UK*
† Applied Psychology Unit, 15 Chaucer Road, Cambridge CB2 2EF, UK
§ Neuroimaging Unit, ‡ Brain Image Analysis Unit, ¶ Department of Psychology, Institute of Psychiatry, De Crespigny Park, London SE5 8AF, UK
‖ School of Psychology, University of St Andrews, Fife KY16 9JU, UK

Recognition of facial expressions is critical to our appreciation of the social and physical environment, with separate emotions having distinct facial expressions[1]. Perception of fearful facial expressions has been extensively studied, appearing to depend upon the amygdala[2–6]. Disgust—literally 'bad taste'—is another important emotion, with a distinct evolutionary history[7], and is conveyed by a characteristic facial expression[8–10]. We have used functional magnetic resonance imaging (fMRI) to examine the neural substrate for perceiving disgust expressions. Normal volunteers were presented with faces showing mild or strong disgust or fear. Cerebral activation in response to these stimuli was contrasted with that for neutral faces. Results for fear generally confirmed previous positron emission tomography findings of amygdala involvement. Both strong and mild expressions of disgust activated anterior insular cortex but not the amygdala; strong disgust also activated structures linked to a limbic cortico–striatal–thalamic circuit. The anterior insula is known to be involved in responses to offensive tastes. The neural response to facial expressions of disgust in others is thus closely related to appraisal of distasteful stimuli.

We aimed to demonstrate distinct neural substrates for perception of two emotions, fear and disgust, replicating previous observations of a link between fear perception and amygdala activation[5,6], and examining the substrate for perception of disgust. It was postulated that perception of facial expressions of disgust would involve structures implicated in the appreciation of offensive stimuli. A cortico–striatal–thalamic circuit has been identified in primates[11], which may be involved in responses to emotive stimuli. There is clinical evidence for the probable involvement of some of these structures in appreciation of disgust: impaired recognition of disgust from facial expressions has been reported both in patients with symptomatic Huntington's disease[12], and presymptomatic carriers of the Huntington's gene[13].

Subjects viewed grey-scale pictures of faces from a standard set[14] depicting disgusted, fearful and neutral expressions. There were two levels of intensity (75 and 150%) for the facial expressions of disgust and fear for each individual face, and one level for the neutral expression, all produced by computer graphical manipulation of the prototype of each expression[15] (Fig. 1). As a neutral face, we used an image with a slightly (25%) happy expression (see Methods). Subjects viewed blocks of emotional (disgusted or fearful) faces alternating with neutral faces in blocks. There were four separate experiments, in a randomized order, incorporating an alternating (neutral/emotional) design for each emotion (fear/disgust) and intensity of expression (mild, 75%; strong, 150%). After presentation of each face, subjects made a decision as to its sex by pressing one of two buttons with the right thumb. The sex decision task was chosen to allow an identical task and response across all conditions, and to permit comparison to a previous study of fear which also

Nature © Macmillan Publishers Ltd 1997

Nature © Macmillan Publishers Ltd 1997